Laser beam evaluation methods to study changes in 12 MeV energetic protons irradiated glasses

M-R IOAN[a], I. GRUIA[c], G-V.IOAN[a], L. RUSEN[b,c], P. IOAN[a], A. ZORILĂ[b,d]
[a]*"Horia Hulubei" National Institute of Physics and Nuclear Engineering - IFIN HH, 30 Reactorului Str., 077125 Măgurele - Bucharest, Romania*
[b]*ISOTEST Laboratory, National Institute for Lasers, Plasma and Radiation Physics, 409 Atomiştilor Str., 077125 Măgurele - Bucharest, Romania*
[c]*Physics Department, University of Bucharest, 405 Atomiştilor Str., 077125 Măgurele - Bucharest, Romania*
[d]*"Politehnica" University of Bucharest, 313 Splaiul Independenței, 060042 Bucharest, Romania*

In most applications, optical windows or lenses are the bridges between the laser systems and the real environment and are often subjected to hostile conditions. The purpose of this work is by applying laser beam diagnosis techniques (two methods) to study changes of transparent glass properties induced by their irradiation with strong ionizing radiation (e.g. the high energy proton irradiation may be used to simulate the damage caused by neutron and gamma irradiation, and this way we avoid the difficulties involved with nuclear reactor irradiations. Basically, we investigated the changes due to the colour centres' or other defects produced by irradiating borosilicate glasses with 12MeV energetic protons. In principle we can expect to changes in the transmittance properties of these glasses and for larger-size induced defects even an increase in their scattering properties, or a change in the spatial profile of the laser beam used as a test beam. Several Tempax glass samples were irradiated using the IFIN-HH- 9MV High Voltage Tandem Van de Graff accelerator irradiation facility at a dose rate of about 1.2kGy/s +/- 8% and an average energy of 12 MeV. Energetic and spatial beam characterizations, according to ISO 11554 and ISO 11146-1 standards, were performed on a low power He-Ne laser beam (linearly polarized), before and after passing the beam through each irradiated glass sample. According to the changes in the glass transmittance, the value of the absorption coefficient was determined for several samples (70.11% relative increase). Spatial beam characterization was performed to see whether or not there are changes in the internal structure of glass samples, shown by the varied values of the beam propagation factor M^2. In our case, the experimental set-up has highlighted a relative decrease of the initial laser beam power of 25, 95% on the entire range of absorbed doses (0÷108) KGy. At the same time we showed a relative increase in the coefficient of propagation (M^2) of 7.16% (geometrical method) and 9.27% (fitting method). The measurements were made with an experimental set-up (He-Ne laser type 25-LHP-151-230, Melles Griot, USA; power-meter type PowerMax-USB UV-VIS, Coherent, USA; beam profiler type GRAS20 with dedicated software BeamGage, Ophir Optronics, USA).

(Received June 10, 2013; accepted November 7, 2013)

Keywords: ISO- Standard, laser beam, He-Ne laser, Optical glass, High proton energy, Degradation of transmission

1. Introduction

Optical materials are playing very important roles in nuclear industry, where they are used under heavy radiations environments. Optical degradation caused by neutrons and gamma can evolve by enriching the knowledge of their degradation mechanisms under nuclear radiations and under the rays are different, and information received is optimal only for a certain period of time because of the optical properties losses. High energy proton irradiations offer a suitable method to simulate the neutron radiation damage [1-3, 11, 12]. Laser systems operating in these extreme conditions action of a laser beam [4]. With a low power He-Ne laser beam (before and after passing through samples) we investigated the changes due to the color centers or other defects produced by irradiating borosilicate glasses with 12MeV energetic protons.

Energetic and spatial beams characterizations according to ISO 11554 and ISO 11146-1 standards are presented [5, 6]. Determinations of spatial beam intensity distributions and of the beam propagation characteristics are important parts of laser applications where beam quality is necessary. The techniques for these laser measurements are presented in ISO standards. These methods include various techniques such as those based on CCD camera. In fig.1 there are shown the power-density distributions of the laser beam, these beam-waist profiles were captured at beam waist location (Z_0).

In conformity to ISO 11146-1 we have measured the spatial parameters of a laser beam considered as having orthogonal symmetry (the x and y directions perpendicular), so simple astigmatic, and subsequently approximated as having rotational symmetry (stigmatic). Measuring energy characteristic features of the same laser beam was performed according to the ISO 11554 standard.

This experiment and the results reported in this paper are the perfect occasions to characterize the performance of a CW He-Ne laser beam propagated through different samples such as our irradiated or non-irradiated glass samples.

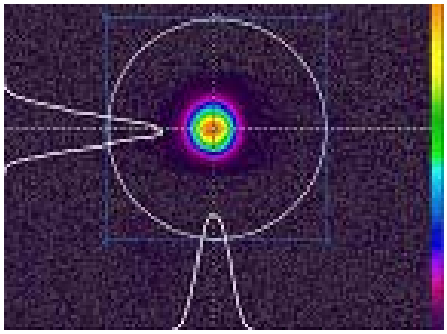

Fig.1a. Beam-waist profile at Z_o -322mm (36 KGy)

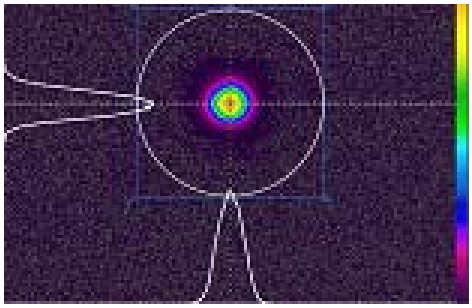

Fig.1b. Beam-waist profile at *Z_o -324mm (72 KGy)*

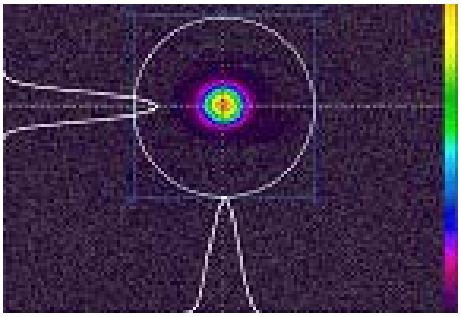

Fig.1c. Beam-waist profile at Z_o -323mm (108 KGy)

The low power laser used in our experiment was intended to avoid the possible laser side-effects on our studied samples. ISO 11146 standard provides measurement procedures to characterize propagation properties of a laser beam. In this standard, the beam diameters are defined by the second-order moments of the power-density distribution, which can be measured with a CCD camera. However, by measuring the power density distribution of the laser beam is critical in the case of a higher amount of beam propagation factor (M2), resulting in a large angle in comparison with a beam divergence close to the diffraction limit. Laser power distribution after passing through irradiated or not-irradiated glasses is related to the lateral extent of power-density distribution of the beam in the measurement plane (z). Therefore, the beam widths of a simple astigmatic beam in x- and y- direction are given by:

$$d_{\sigma x} = 4\sigma_x;\ d_{\sigma y} = 4\sigma_y$$

The space propagation law for the second-order-moment beam diameter is:

$$d^2_i(z) = d^2_{\sigma o} + \theta^2(z_i - z_o)^2 \qquad (1),$$

where d_i is the beam diameter at the location Z_i. At the waist ($z=z_o$), the beam reaches its minimum diameter d_o, and with increasing distance from the waist (z_o), it status spreading with the divergence angle (θ). The transverse propagation properties of any stigmatic beam are fully described by the beam waist d_o, the distance from the waist z_o and the divergence angle θ. The laser beam propagation factor M^2 is defined as the ratio of the products of divergence angle and beam waist of the measured beam to the product of the fundamental beam:

$$M^2 = (\pi/4\lambda)d_o\theta.$$

The beam propagation factor of the fundamental modes TEM_{oo} is 1, and for real beam is over 1. The propagation of a simple astigmatic beam can be expressed by two analogous expressions to equation (1), which describe the propagation along the two principal axes of the beam ($d_{o,x}$, $d_{o,y}$, θ_x, θ_y, $z_{o,x}$, $z_{o,y}$). The combined determination of beam propagation parameters according to ISO standards has to be performed by recording spatial propagation parameters of the beam widths under the influence of irradiated samples.Measurement system uses a beam profiler type GRAS20 with dedicated software (BeamGage - Ophir Optronics) to measure the beam intensity distribution. To avoid introducing aberration into the beam, a minimum number of optical components were used to attenuate the laser intensity and a long focal length plan-convex lens was used to create the beam waist in space. Only a single lens was used to create a waist for spot-size measurements to minimize measurement errors in the location of the beam minimum waist location and cavity distance from the lens.

2.Technical irradiation process

Proton beam intensity and irradiation times were set in order to obtain total absorbed doses of 36, 72 and respectively 108KGy, trying to avoid unwanted radioactive activation of our samples.

Proton irradiations have been performed at Bucharest 9MV-HVEC Tandem Van de Graff accelerator. The 12MeV proton irradiations were carried out in air by extracting the beam through a 40μm Al foil, and then passing 20mm of air to the samples from 12.4MeV. For all the proton irradiations the average intensity was about

$3*10^{10}$ p/s and at an approximately 5mm beam diameter. The samples were held at the edges in a rigid support and the temperature was monitored by a K-type thermocouple attached to the edge of the back face. During irradiations the indicated temperature was about 40°C and this way we simulated the self-heating effect of the laser beam propagation through our samples. We used 4 Tempax samples with average thickness of 2mm. Because glass is an insulating material it is difficult to align the beam on target. The solution found was to place in front of the sample of a metal sensor (smaller than the sample surface) with which we have measured proton currents that passed through Al foil and air before reaching the target. An optimal aligned beam on a sample it is considerate when the current value measured on the sensor is maximum, while the last collimator measured current value is minimal. After alignment, the sensor is removed from the sample and the irradiation runs to normal. We have used the 12MeV protons beam carefully, because a certain amount of radioactivity is induced in samples in the time of irradiations. Thirty days after the end of the irradiation, samples are practically non-radioactive and could be measured in terms of good radioprotection [7].

Before irradiation procedure, at 12MeV protons, we have simulated the depth of penetration for all glass samples and calculated the ratio of Tempax energy loss by electronic and nuclear collisions, using Monte Carlo simulation program SRIM 2008 [8]. Estimated protons beam penetration depth in the Tempax samples is about 935µm, and the ratio of energy loss by electronic and nuclear interactions is about 2063. This means that the main component of the stopping power in this case is the electronic one. We have focused on dissymmetric aspects, determining the supplementary irradiation doses induced by the proton through emitted neutrons and gamma radiations. The proton dose it is theoretically calculated on the ratio between the energy given by the duration of the irradiation beam (beam diameter in the cylinder volume and depth of penetration of the sample) and the equivalent mass of that volume (1J/kg = 1Gy).

3. Measuring the output power of the laser beam after passing through the sample.

The most important method of testing the performance of a laser system is to measure its power output. Output power directly affects laser's ability to perform a certain process after passing through an irradiated glass. Results were obtained with a power meter type PowerMax-USB UV-VIS. Measuring this parameter is often very important from the time a laser is manufactured and to the final end customer who will be using the laser system in nuclear applications. Fig. 2 shows the measurement of laser's output power after passing through irradiated glasses.

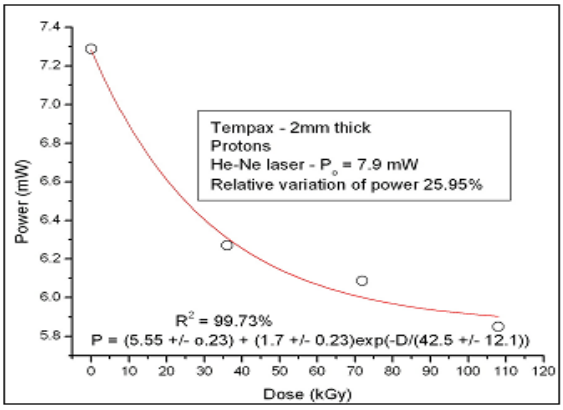

Fig.2 shows the variation of output power after passing through irradiated glasses vs. dose level.

These types of measurement systems are composed by a sensor that is placed into the laser beam after passing through samples and provides an output signal proportional to the initial laser output and a meter attached to it, which is an analyzer that will display and interpret the signal from the sensor. The power of a laser is measured in Watts and often reported in terms of nW or mW. This is referring to the optical power output of continuous wave (CW) lasers. From the data obtained, we determined the variation of the absorption coefficient in measured samples as we can see in Fig. 3.

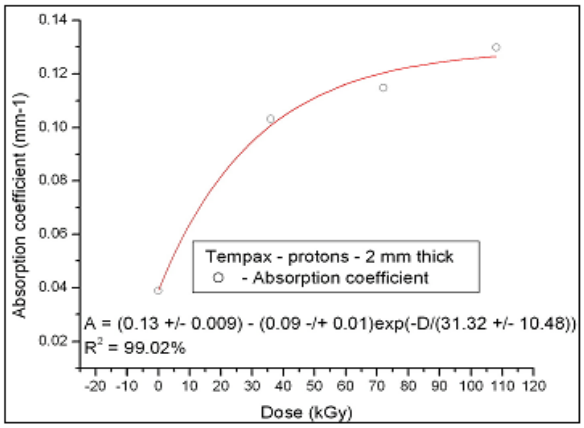

Fig.3 shows the absorption coefficient.

These data indicate an increase in the absorption coefficient of about 70% compared to non-irradiated sample vs. dose level.

The irradiation was performed at a temperature of 40°C and that is way the migration of color centers have a patchy distribution in the adjacent proton beam incident surface (5mm diameter). In Fig. 4 it is shown the spatial distribution of the optical transmission in irradiated samples (x and y - perpendicular directions).

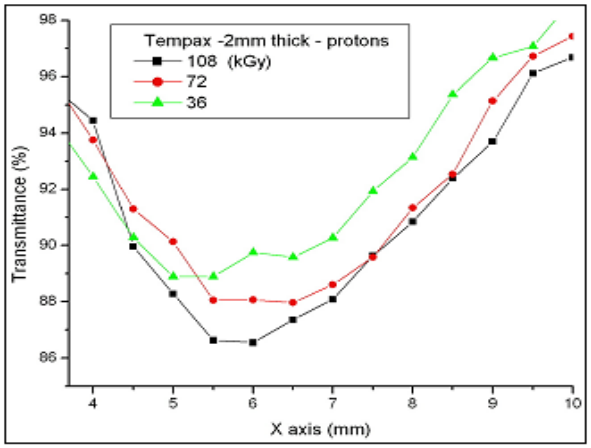

Fig.4.a shows the spatial distribution of the optical transmission in irradiated samples (x - direction).

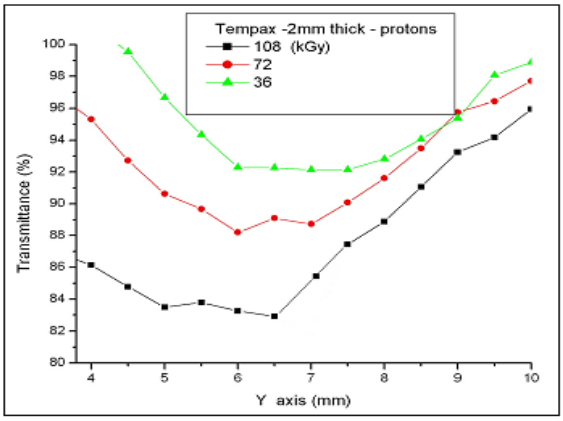

Fig.4.b shows the spatial distribution of the optical transmission in irradiated samples (y - direction).

4. Experiment

A schematic representation of the optical configuration used in performing these measurements is shown in Fig.5.

The raw output power from the laser is passed through our glass samples, the optical attenuators, the two mirrors reflecting more than 99.9% and changing the direction of the beam (180^{o}) and then enters in the focusing lens and in the CCD camera. These optical elements were used to attenuate the laser power by a factor of approximately 27 and reduce the ghost beam intensity, due to secondary reflections, to below detectable levels. This attenuation brought the beam down to nW levels where neutral density filters could be safely used to perform the final attenuation of laser beam to within the linear range of the detector array. A total optical attenuation of the beam of 7.9mW to 0.3mW was required to reduce the focal beam intensity to usable levels on the CCD array.

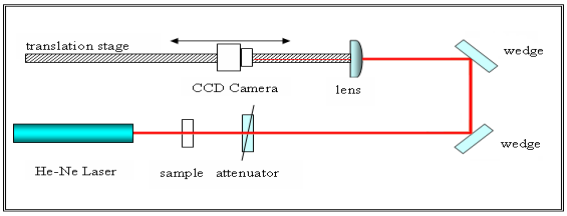

Fig.5.a shows optical scheme of the set-up.

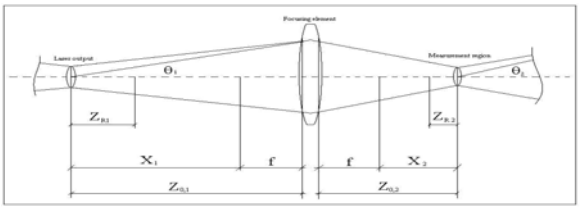

Fig.5.b shows a more complex diagram involving all the necessary parameters to characterize the beam geometry.

The first method (geometrical method) was similar to that described in the proposed ISO standard for beam parameter measurement [6, 9]. The minimum spot diameter and a second beam diameter along the optical axis, as well as the position of the waist creating lens were extracted from each data set. These values were input to a mathematical analysis software package according to the Table 1 (first column).

The measured beam diameter data at various positions along the optical lens created waist for irradiated glasses are given in Fig.6.

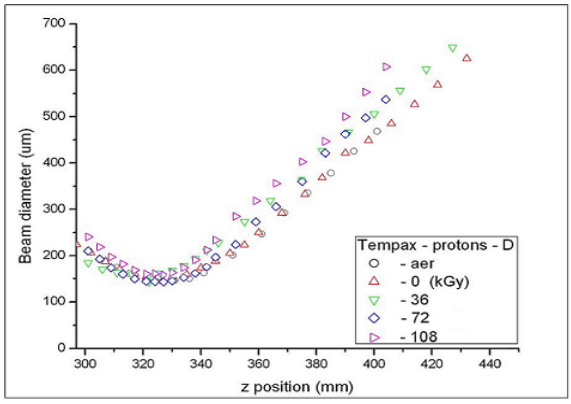

Fig.6 shows illustration of the measured beam diameters of the laser beam (stigmatic) on the dose range (0÷108)KGy vs. propagation distance Z.

The results of the measured data (the assumption simple astigmatic beam) for each condition of total dose are represented in Fig. 7.

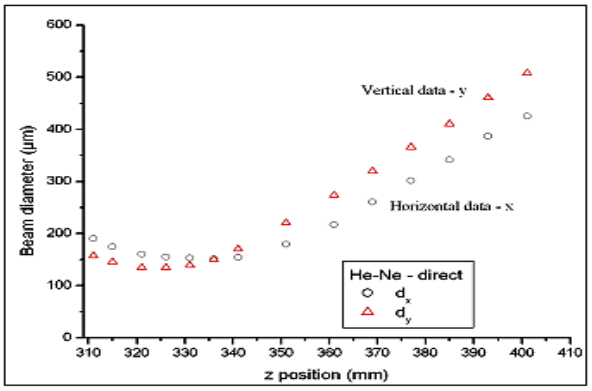

Fig.7a .shows illustration of the measured beam diameters of the laser beam (simple astigmatic) on the air.

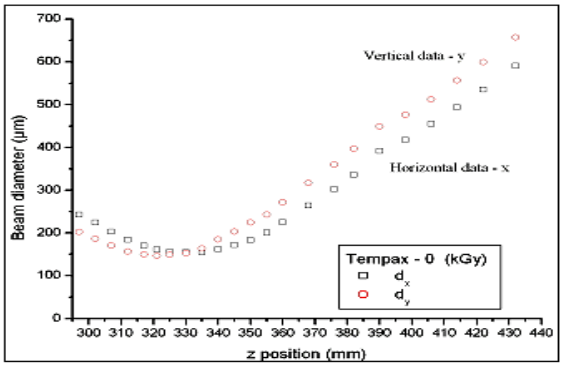

Fig.7b. shows illustration of the measured beam diameters of the laser beam (simple astigmatic) on the dose 0KGy.

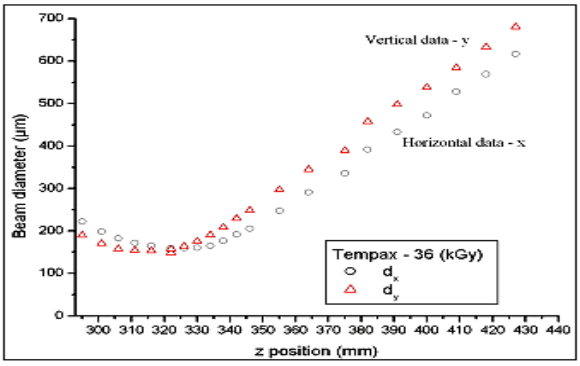

Fig.7c. shows illustration of the measured beam diameters of the laser beam (simple astigmatic) on the dose 36KGy.

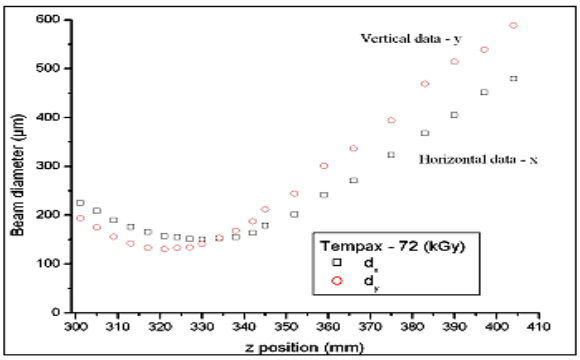

Fig.7d. shows illustration of the measured beam diameters of the laser beam (simple astigmatic) on the dose 72KGy.

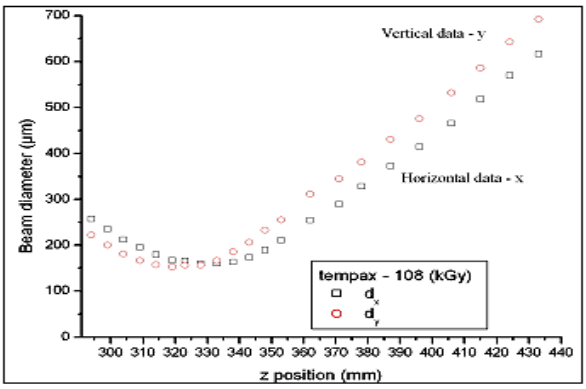

Fig.7e. Shows illustration of the measured beam diameters of the laser beam (simple astigmatic) on the dose 108 KGy.

The second method (fitting method) of determining the beam parameters from the laser, after focusing, involved using a curve fitting routine to fit all of the points of each data set to below equation [6, 10]. All parameters were obtained from performing a hyperbolic fit to the measured beam diameters along the beam propagation axis:

$$d^2_i(z) = a + bz_i + cz_i^2 \qquad (2),$$

were d^2_i is the beam diameter at the location Z_i and a, b, c are the hyperbola parameters. Relation (2) is the propagation equation: $d_i^2 = d_o^2 (1 + \theta_2 (Z_i - Z_o) 2)^2$.

For both methods, the optimal physical parameters of the beam before the focus were determined using these relations:

$$d_{0,1} = d_{0,2}\, V$$
$$(V = f/L^{0,5} \quad L = z^2_{R2} + x_2^2)$$
$$Z_{R1} = V^2 Z_{R2}$$
$$\theta_1 = \theta_2/V$$
$$X_1 = V^2 X_2$$
$$Z_{o,1} = X_1 + f$$

Relations that give the physical parameters of the beam after focusing and anterior focus are presented below.

Table 1 - Shows relations calculator physical parameters for the laser beam by the two methods.

Geometrical method	Fitting method
$Z_{0,2}$	$Z_{0,2} = -b/2c$
$d_{0,2}$	$d_{0,2} = [(4ac - b^2)/4c]^{0.5}$
$\theta_2 = d_{0,2}/Z_{R2}$	$\theta_2 = c^{0.5}$
Z_{R2}	$Z_{R2} = [(4ac - b^2)/4c^2]^{0.5}$
$M^2 = \pi\, d_{0,2} /(4\lambda Z_{R2})$	$M^2 = \pi[(4ac - b^2)]^{0.5}/8\lambda$
$X_2 = Z_{0,2} - f$	f = 281.81mm

5. Results and discussions

Over the plots of the beam data in this figure, there are displayed the numerical values for the beam parameters obtained from the curve routine (a, b, c) – Table 2 and from hyperbolic fit equation – Table 4. With their help and relationships from the Table 1 (second column) are calculated propagation parameters after focusing lens.

Table 2. The hyperbola fit parameters:(a, b, c) - stigmatic beam (a_x, a_y b_x, b_y) - simple astigmatic beam.

Dose (KGy)	Air	0	36	72	108
a ($x10^6$)	3.95+/-0.19%	3.47+/-0.998%	4.61+/-0.85%	3.49+/-1.08%	3.64+/-0.34%
b ($x10^3$)	24.04+/-0.2%	21.17+/-0.99%	28.28+/-0.87%	21.78+/-1.1%	22.31+/-0.34%
c	36.74+/-0.12%	32.54+/-0.99%	43.56+/-0.86%	34.23+/-1.09%	34.38+/-0.33%
Fitting parameters – laser beam approximated stigmatic					
a_x ($x10^6$)	3.68+/-0.39%	3.48+/-0.92%	3.74+/-0.69%	3.47+/-0.99%	3.59+/-0.29%
b_x ($x10^3$)	26.04+/-0.25%	21.37+/-1.08%	22.2+/-1.02%	31.63+/-1.34%	22.89+/-0.43%
c_x	33.3+/-0.43%	31.75+/-0.93%	33.17+/-0.71%	37.88+/-1.03%	32.99+/-0.29%
Fitting parameters – simple astigmatic laser beam in the x direction					
a_y ($x10^6$)	4.23+/-0.24%	3.45+/-1.09%	35.1+/-1.02%	5.1+/-1.34%	3.69+/-0.43%
b_y ($x10^3$)	26.04+/-0.25%	21.37+/-1.08%	22.2+/-1.02%	31.63+/-1.34%	22.89+/-0.43%
c_y	40.24+/-0.24%	33.32+/-1.04%	35.34+/-0.95%	49.21+/-1.32%	35.75+/-0.41%
Fitting parameters – simple astigmatic laser beam in the y direction					

The beam parameters are then obtained from a hyperbolic fit to the measured data. Because the achievable accuracy of the beam parameters strongly depends on the number and positions of the measurement planes with respect to the beam waist, ISO 11146 gives detailed provisions. At least five measurement planes should be near the beam waist (within one Rayleigh range) for accurately determining the waist diameter. At least five additional measurement planes in a distance more than two Rayleigh lengths away from the beam waist are necessary for accurate determination of divergence angle and waist position. If the measurement planes are arranged nearly symmetrically around the beam waist, the accuracies can be further increased.

A 14-bits CCD camera was used to capture the power-density distributions of a simple astigmatic beam (Fig. 1). An almost circular and smooth power-density distribution was measured at the beam waist. At distances of about one Rayleigh length away from the waist, the beam profile is almost constant. The relative deviations of the measured beam diameters to the fitted parabola are less than 5 percent (Table 3). Using this characterization technique, it is possible to describe the complete beam propagation behavior and the optical focusing of such beams in an elegant manner.

The diameter measurements and their relative positions according to the waist creating lens were then used in predicting the laser beam characteristics. The results of these calculations are given in Table 3.

Table 3a. - parameters defining simple astigmatic laser beam after focusing (geometrical method (M_1) and fitting method (M_2) - computed with the Table 1 column 1, 2, custom perpendicular directions x and y).

Dose (KGy)		Air	0	36	72	108	Relative variation(%)
M^2_x	M_1	1.08+/-3.15%	1.08+/-3.15%	1.12+/-2.13%	1.14+/-2.83%	1.13+/-1.42%	11.58+/-5.1%
	M_2	1.048+/-1.18%	1.093+/-3.88%	1.131+/-1.65%	1.1458+/-0.29%	1.133+/-0.49%	8.54+/-1.25%
M^2_y	M_1	1,07+/-3.75%	1.07+/-3.75%	1.12+/-3.38%	1.13+/-5.19%	1.15+/-2.3%	6.96+/-4.96%
	M_2	1.049+/-0.74%	1.095+/-1.92%	1.167+/-1.83%	1.156+/-0.48%	1.159+/-0.74%	10.11+/-1.2%
Z_{R2} x	M_1	27.04+/-1.63%	27.04+/-1.6%	27.38+/-1.1%	24.12+/-1.49%	27.51+/-0.7%	12.32+/-1.7%
	M_2	25.387+/-0.8%	27.76+/-2.1%	27.49+/-1.96%	24.388+/-1.14%	27.68+/-0.79%	12.15+/-3.1%
Z_{R2} y	M_1	25.5+/-1.91%	25.5+/-1.9%	25.41+/-1.7%	18.35+/-2.57%	25.73+/-1.16%	28.68+/-3.0%
	M_2	21.03+/-0.78%	26.5+/-2.18%	28.223+/-2.0%	18.947+/-1.4%	26.15+/-0.84%	32.87+/-3.2%
$Z_{0,2}$ x	M_1	330.28+/-1.6%	330.28+/-0.0%	326.9+/-0.08%	329.1+/-0.08%	327.97+/-0.0%	1.02+/-2.3%
	M_2	331.58+/-0.4%	330.27+/-1.4%	320.66+/-1.2%	328.93+/-1.69%	329.5+/-0.5%	0.8+/-1.38%
$Z_{0,2}$ y	M_1	320.7+/-0.09%	320.7+/-0.1%	318.4+/-0.1%	321.66+/-0.11%	319.02+/-0.0%	1.01+/-0.18%
	M_2	323.58+/-0.3%	320.65+/-1.4%	314.11+/-1.6%	321.34+/-1.88%	320.17+/0,5%	2.93+/-1.67%
$d_{0,2}$ x	M_1	153.17+/-1.3%	153.17+/-1.3%	157.23+/-1.1%	148.59+/-1.2%	158.24+/-0.6%	6.09+/-1.47%
	M_2	146.38+/-1.1%	156.43+/-3.9%	158.34+/-1.6%	150.12+/-0.59%	159.04+/-0.5%	7.96+/-11.2%
$d_{0,2}$ y	M_1	148.22+/-1.6%	148.22+/-1.6%	151.56+/-1.4%	129.12+/-2.25%	154.19+/-0.9%	16.26+/-2.6%
	M_2	133.41+/0.7%	152.99+/1.9%	158.29+/-1.8%	132.93+/-0.82%	156.38+/-0.7%	16.22+/-2.7%
θ_{2x}	M_1	5.74+/-0.94%	5.66+/-2.11%	5.74+/-1.43%	6.16+/-1.92%	5.75+/-0.95%	8.12+/-3.43%
	M_2	5.77+/-0.2%	5.64+/-0.46%	5.75+/-0.35%	6.15+/-0.5%	5.74+/-0.14%	8.29+/-0.84%
θ_{2y}	M_1	5.81+/-2.5%	6.18+/-1.28%	5.96+/-2.24%	7.04+/-3.42%	5.99+/-1.53%	17.47+/-5.4%
	M_2	6.34+/-0.12%	5.77+/-0.5%	5.95+/-0.47%	7.02+/-0.65%	5.97+/-0.2%	17.8+/-1.05%

Table 3.b - parameters of the laser beam after focusing stigmatic (geometrical method (M_1) and fitting method (M_2) - computed with the Table 1 column 1, 2).

Dose (KGy)		Air	0	36	72	108	Relative variation (%)
M^2	M_1	1.075+/-1.14%	1.09+/-3.29%	1.139+/-2.54%	1.15+/-1.66%	1.16+/-2.83%	7.16+/-4.16%
	M_2	1.072+/-0.52%	1.11+/-1.56%	1.16+/-2.48%	1.15+/-1.8%	1.18+/-0.73%	9.27+/-1.16%
Z_{R2} (mm)	M_1	23.62+/-0.57%	26.71+/-1.7%	26.74+/-1.29%	21.37+/-1.85%	27.01+/-0.8%	20.88+/-2.17%
	M_2	23.53+/-0.53%	27.55+/-1.85%	27.49+/-2.58%	21.81+/-2.13%	21.87+/-0.79%	20.83+/-3.37%
$Z_{0,2}$ (mm)	M_1	326.23+/-0.0%	325.36+/-0.0%	322.47+/-0.0%	324.86+/-0.0%	323.3+/-0.05%	1.15+/-0.07%
	M_2	327.2+/-0.23%	325.35+/-1.4%	318.16+/-1.2%	324.65+/-1.4%	324.65+/-0.3%	2.76+/-1.26%
θ_2 (mrd)	M_1	6.057+/-0.76%	5.737+/-2.2%	5.853+/-1.69%	6.613+/-2.4%	5.871+/-1.11%	13.16+/-3.8%
	M_2	6.061+/-0.6%	5.704+/-0.49%	5.851+/-0.43%	6.599+/-0.5%	6.599+/-0.16%	13.56+/-0.54%
$d_{0,2}$ (μm)	M_1	143.06+/-0.4%	153.26+/-1.4%	156.51+/-1.0%	141.29+/-1.5%	158.54+/-0.7%	7.98+ /-1.85%
	M_2	142.63+/-0.5%	157.14+/-1.6%	160.86+/-2.4%	143.92+/-1.9%	144.37+/-0.7%	11.33+/-3.53%

Used fit hyperbola equations are presented below:

Table 4 - The fit hyperbola equations - stigmatic beam (second) and simple astigmatic beam (the third) column.

Dose (kGy)	Fitting hyperbola relations	
	For laser beam with circular symmetry (stigmatic)	For asymmetric geometry laser beam perpendicular directions x and y (simple astigmatic)
Air	$d^2 = 3.96*10^6 - 24.1*10^3 Z + 36.77 Z^2$	$d^2_x = 3.68*10^6 - 22.1*10^3 Z + 33.3 Z^2$
		$d^2_y = 4.23*10^6 - 26.04*10^3 Z + 40.24 Z^2$
0	$d^2 = 3.47*10^6 - 21.17*10^3 Z + 32.54 Z^2$	$d^2_x = 3.49*10^6 - 20.97*10^3 Z + 31.75 Z^2$
		$d^2_y = 3.45*10^6 - 21.37*10^3 Z + 33.32 Z^2$
36	$d^2 = 3.49*10^6 - 21.78*10^3 Z + 34.2318 Z^2$	$d^2_x = 3.47*10^6 - 21.39*10^3 Z + 33.17 Z^2$
		$d^2_y = 3.51*10^6 - 22.2*10^3 Z + 35.35 Z^2$
72	$d^2 = 4.61*10^6 - 28.2*10^3 Z + 43.56 Z^2$	$d^2_x = 4.12*10^6 - 24.92*10^3 Z + 37.89 Z^2$
		$d^2_y = 5.09*10^6 - 31.63*10^3 X + 49.22 Z^2$
108	$d^2 = 3.64*10^6 - 22.31*10^3 Z + 34.38 Z^2$	$d^2_x = 3.59*10^6 - 21.71*10^3 Z + 32.99 Z^2$
		$d^2_y = 3.69*10^6 - 22.89*10^3 Z + 35.75 Z^2$

Numerical values for the beam quality factor M^2 were obtained by two different procedures.

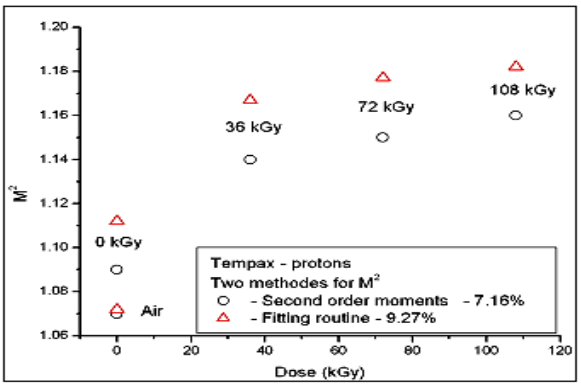

Fig.8 shows propagation parameter (M^2) by the two methods vs. dose level.

However, difference in the M^2 values do exist at various total absorbed doses, in particular at 0, 36, 72 and 108KGy. At these doses levels the values of M^2 vary approximately 7.16% and respectively 9.27%.

6. Conclusions

Our work was focused on the diagnosis of a He-Ne laser beam (linearly polarized) after passing through our glass samples (Tempax) which were optical affected by irradiation with high-energy protons and after focused on a CCD camera plan. The effect of optical degradation of irradiated samples (0-108) kGy was highlighted by: a relative increase in the absorption coefficient variation (approximately 70%), a lower initial power relative variation (approximately 25%) and a relative variation propagation coefficient of about 7% for the geometric method and approximately 9% fidelity for the fitting method.

These results were obtained by measuring four Tempax glass samples (irradiated with 12MeV proton energy) to total absorbed dose levels of 0, 36, 72 and 108 (KGy).

The two methods used in the processing of information were based on theoretical, experimental and calculated values in accordance with ISO standards in use.

Measurements were performed, first, in the assumption of a simple astigmatic beam (asymmetric geometry perpendicular directions x and y) and then it was approximated by a stigmatic laser beam (circular geometry).

The relative errors for the parameters used in the diagnosis are below 5%, which shows that these ISO standards could be applied in this case accurately.

Using a low-power laser (7.9mW) took into account the possible changes in diagnostic parameters to be due only the accumulated dose effects, and no side effects caused by the laser beam.

Next, we consider the implementation of an experimental set-up (power laser pulse) to test the behavior of the laser beam (the passage through irradiated samples) on samples of 304-type stainless steel placed in the beam focusing plane [4].

Acknowledgements

We would like to thank to Dr. G. Nemes and Dr. A. Stratan, ISOTEST Laboratory, National Institute for Lasers, Plasma and Radiation Physics for optical measurements and for the required time for clarification and discussion. We also thank to the Department of Nuclear Physics (DFN-TANDEM) of IFIN-HH to provide technical assistance to irradiation.

References

[1] B. Constantinescu, R. Bugoi, P. Ioan, L. Radulescu, M. Brasoveanu, M. Dragusin, Romanian Journal of physics, **48**, 355 (2003).
[2] S. Baccaro, A. Piegari, I.Di. Sarcina, A. Cecilia, IEEE Transmission on Nuclear Science, **52**, N5 (2005).
[3] B. Constantinescu, R. Bugoi, E.R. Hodgson, R. Vila, P. Ioan, Journal of Nuclear Materials, B **367-370**, 1048 (2007).
[4] I. Avarvarei, O. Dontu, D. Besnea, I. Voiculescu, R. Ciobanu, Optoelectron. Adv. Mater.-Rapid Commun. **4(**11), 1894 (2010);
[5] ISO 13694, Test methods for laser beam parameters: Power (energy) density distribution;
[6] ISO 11146, Test methods for laser beam parameters: Beam widths, divergence angle and beam propagation factor;
[7] Se-Jin Ra, Kye-Ryung Kim, Myung-Havan Jung, Journal of the Korean Physical Society, **56(**6), 2093 (2010).
[8] www.srim.org./TRIM/SRIM2008;
[9] D. M. Keicher, SPIE proceedings, **2375**, 161 (1995).
[10] J.V. Sheldakova, A.V. Kudryashov, V.Y. Zavarova, T.Y. Cherezova, SPIE proceedings, vol.6452-2007;
[11] M -R. Ioan, I. Gruia, P.Ioan, I. L. Cazan, C. Gavrila, J. Optoelectron. Adv. Mater., **15**(3 – 4), 254 (2013).
[12] M.-R. Ioan, I. Gruia, P. Ioan, M. Bacalum, G.-V. Ioan, C. Gavrila, J. Optoelectron. Adv. Mater. **15**(5), (2013) in press

*Corresponding author: gruia_ion@yahoo.com

ANNEX - Gamma spectra measured after the irradiation with high-energy protons

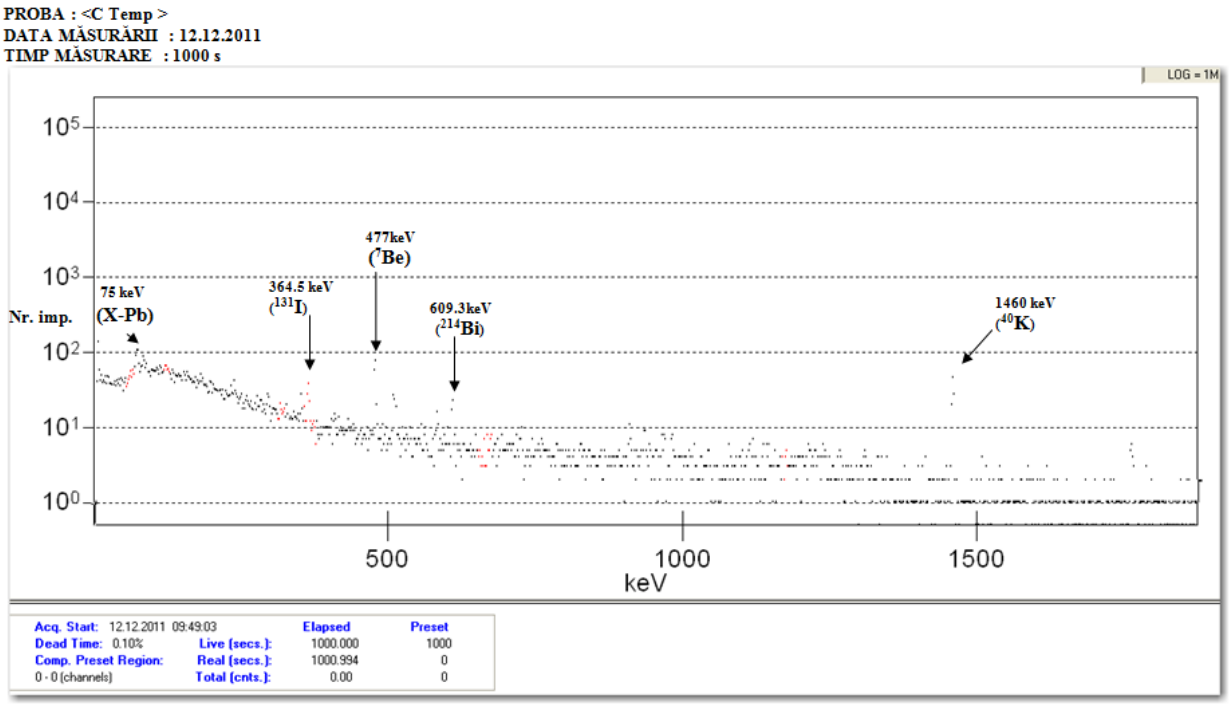

Samples were analyzed with a complex gamma spectrometric chain containing: a HPGe (Hyper Pure Germanium) semiconductor detector type GC 2520 - 7500 SL, a multichannel analyzer type Canberra MP2 - 1E - Multiport II, a HV power supply type 2861, an amplifier type model 2024, a preamplifier type 2002 CSL, a cooling system and an attached PC. The appendix shows a reduced number of active elements, but also a reduced amount of activity (equivalent in cps). The "active" elements values found are below 10^2cps.